Biomedical Engineering Advances 2 (2021) 100008

Contents lists available at ScienceDirect

Biomedical Engineering Advances

journal homepage: www.elsevier.com/locate/bea

ECG-based biometric recognition under exercise and rest situations

Wei Cui*, Zihan Wang, Yaoguang Li

School of Automation Science and Engineering, South China University of Technology, Guangzhou 510641, China

ARTICLE INFO

Keywords:
Human identification
ECG database
Biometric recognition
KL divergence
Deep learning

ABSTRACT

As a core technology in the field of information security, human biometric recognition has become the focus of researchers' attention during the past few years, which is based on a myriad of biometric features including fingerprint, face, retina, etc. Due to the high difficulty of forgery, electrocardiogram (ECG) has a great potential to be applied into identification, while merely experiments on its rest situation have been worked on. In this manuscript, we overcome the oversimplification of previous researches, build our own ECG dataset containing signals under both exercise and rest situations, and evaluate the resulting performance on ECG human identification (ECGID), especially the influence of exercise on the whole experiment. By applying several established learning algorithms to our own ECG dataset, we find that current methods which can well support the identification of individual under rests, cannot equally present satisfying performance under exercise situations, therefore exposing the deficiency of existing ECG identification algorithms.

1. Introduction

With the increasing demand for high information security which are occasionally considered vulnerable to fabrication and spoofing attacks, reliability of protective methods has become an important research topic in corresponding field. However, traditional identification technologies such as certificates and passwords which are likely to be forgotten and stolen, put the personal information in jeopardy, thus no longer meet the requirement for security. At the same time, based on individual's unique anatomical, physiological or behavioral characteristics which are virtually impossible to be forged, biometric identification technology has emerged. Even though the common and sophisticated biometric features [1–5] including face, fingerprint and voice, have high recognition rates so far, they are not perfect enough. For example, a FaceID can be corrupted by photograph modification or make-up; a fingerprint can be copied and recreated with latex; a voice can be recorded then imitated as well. In order to strengthen the security of such identification technology, some scholars combine multiple biometric technologies with each other to make systems harder to be cracked, others have been trying new techniques since 20 years ago, such as ECGID which we can guarantee its reliability by generating from living bodies [6–8]. Regarding to the uniqueness of ECG to individual, several researches have verified it using different approaches, therefore provides us a theoretical basis for ECG-based human identification [9,10].

Containing abundant information about individual identity, ECG waveform has four fundamental characteristics required for biometric identification [11]: (1) Universality: the heart of every living human generates ECG signals all the time; (2) Uniqueness: the ECG differences between individuals are mainly affected by body shape, age, weight, emotion, gender, heart location, heart size, geometric shape, physiological characteristics, chest structure and sports status, etc., determining the Uniqueness of ECGs generated by different people [12]; (3) Stability: the structure and size of the adult heartbeat are basically fixed and ECG waveforms remain stable unless one's heart exists lesions; (4) Measurability: with miniaturization, portability and high precision, ECG equipment is able to reduce the cost and time of ECG acquisition and thus makes the measurement more convenient. In recent years, ECG signal has become the focus of major research in the field of human identification technology due to its excellent non-replicability and uniqueness. The methods of ECGID can be divided into two categories: (1) Fiducial approach: as shown in Fig. 1, ECG signal is composed by three main waves, the P, QRS and T waves [13,14], and each peak, slope, boundary and interval are depicted by Fiducial features, which are utilized for human identification by the fiducial method; (2) Non-fiducial approach: these methods treat ECG signals as a whole without taking into consideration the details of waveform, and process signals in the frequency domain in most cases.

Biel et al. extracted 30 time and amplitude features and selected 21 features to form the eigenvector with correlation matrix analysis [10], demonstrating that soft independent modelling of class analogy method is implemented for classification. Israel et al. located the key points by finding the local extremum of the waveform in each heartbeat and extracted 15 features to classify subjects through linear discriminant analysis [15]. This experiment included 29 subjects, with the identification accuracy reaching 100% and heartbeat recognition accuracy reaching

* Corresponding author.
E-mail address: aucuiwei@scut.edu.cn (W. Cui).

https://doi.org/10.1016/j.bea.2021.100008
Received 12 June 2021; Received in revised form 19 July 2021; Accepted 22 July 2021
Available online 31 July 2021

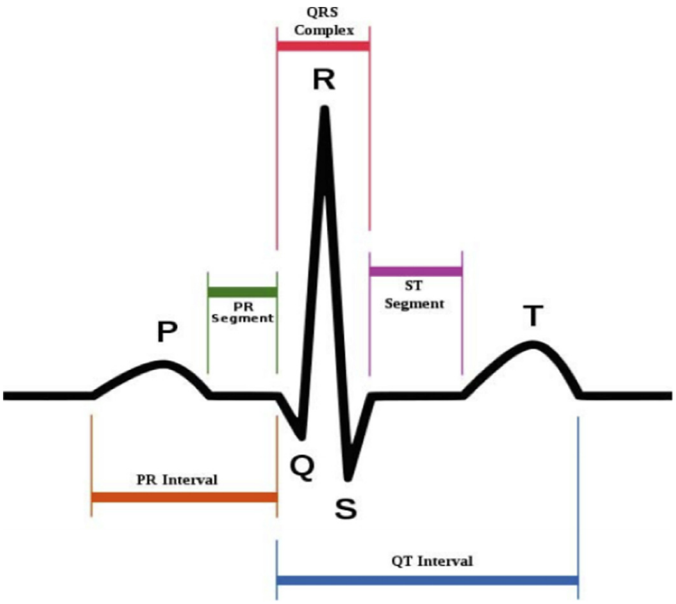

Fig. 1. A real time ECG signal [13].

81%. Saechia et al. adopted Fourier coefficients to examine the effectiveness of segmenting ECG heartbeat [16]. Shen et al. proposed an identification method based on one-lead ECG [17] and obtained 7 time domain features from QRS complex. They used template matching and decision-based neural network to complete the verification, with 100% correct verification accuracy. Plataniotis et al. first introduced an ECG biometric recognition method requiring no waveform detection and analyzed the auto-correlation of ECGs while applying DCT to achieve dimensionality reduction [18]. Wang et al. followed the AC-DCT method and achieved satisfying results [19]. Agrafioti et al. combined the autocorrelation and LDA to make the classification [20]. Although the above literatures have obtained good performance, there remains some important problems that cannot be overlooked, such as robustness of ECGID including, (1) heart disease: one was enrolled in good heart health, but tested under the condition of heart disease; (2) emotion: one was enrolled in calm, but tested in emotional state; (3) exercise: one was enrolled in rest, but tested after exercise which we call the rest-ex ECGID. Some researchers [21,22] have explored the first question with the MIT-BIH database [23] or the PTB database [24], but the latter two issues have rarely been studied. Therefore, we would like to discuss the third issue in this manuscript, that is, the robustness of rest-ex ECGID.

From the 1970s to the 1990s, some researchers [25–28] attempted to dig out the changes of ECG waveform between rest and exercise, showing that during exercise the amplitude of P wave increases while that of T wave decreases, and the QRS duration remains nearly constant. During the first minute after exercise, the amplitude of P and T wave both increase and other features such as P and T wave start to return to normal. However, they only got qualitative results, not quantitative ones. Afterwards, the literature on the effects of exercise on ECGID appears, but few satisfying results on rest-ex ECGID have been achieved since post-exercise is a period of recovery where various features change abruptly. Kim et al.[29] discussed the effects of exercise on QRS interval, RT interval and QT interval, used inverse Fourier transform to normalize features and improved rest-ex ECGID performance. Poree et al.[30] used correlation coefficient for template matching to find out the effects of exercise, waveform length and the number of leads on ECGID. Piao et al.[31] collected ECG records of only 5 normal people in rest and movement states. They used discrete wavelet transform for feature extraction, Euclidean distance and nearest neighbour for classification, with an accuracy of 100%. Sung et al.[32] collected ECG data of 55 subjects before and after exercise for 5 min respectively. The first and

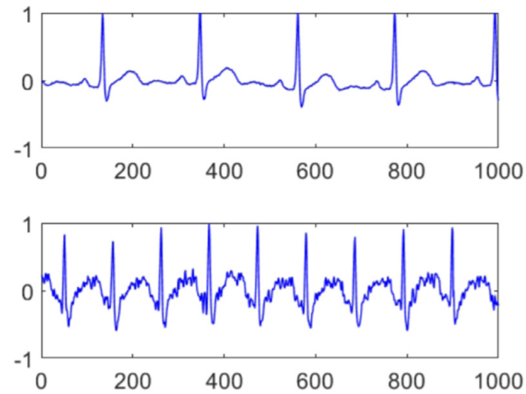

Fig. 2. Subject 1's ECG records before and after exercise.

second order differential of waveform were used to help feature point detection. LDA is a method for feature extraction and classification, with the accuracy of identification being 59.64% within 1 min after exercise, and more than 90% beyond 1 min. It needs to be tested with more advanced AI methods. Nobunaga et al.[33] showed that after bandpass filtering between 10 Hz and 80 Hz, the ECG waveforms in rest and post-exercise would be highly similar, and the rest-ex ECGID rate achieved 99.7% on 10 subjects. Komeili et al.[34] extracted different types of features and used feature selection algorithms to select the most stable ones in exercise. Recently, Ref[35]. designed a biometric system to operate in either verification or identification mode. The performance of the proposed scheme was evaluated using the ECGs of 287 subjects. However the robustness of the test is not considered.

This manuscript is aimed at applying existing methods to analyse the performance of rest-ex ECGID with our ECG dataset [36]. Through multiple sets of experiments, we find that for current methods, the rest-rest ECGID accuracy can reach more than 95% while both training and resting on the exercise dataset (the ex-ex ECGID) performance become a little worse; As for the rest-ex ECGID performance, most methods collapse to 10% or even worse, except for the KL feature selection method, which can reach almost 65%. Although compared with other methods the KL feature selection method performs much better, its result still remains unsatisfactory.

2. Experiment

2.1. Database

Since neither the widely used MIT-BIH database nor the PTB ECG database contain data specifically targeted for ECG identification, we built our own dataset with the support of student volunteers recruited by our research group in Prof. Cui's laboratory at South China University of Technology [36]. The database includes pre and post exercise recordings for 45 volunteers involving 33 males and 12 females ranging in age from 18 to 22. The ECG signals were captured in lead II whose sampling frequency is set as 300 Hz. The length of recordings in rest and post-exercise condition are around 5 min and 150 s respectively.

During the process, each subject performed a few basic workouts such as running, full squatting or climbing the stairs to speed up their heart rate recorded as data under post-exercise condition ranging from 90 to 150 bpm, while sitting sedentarily to remain their heart rate around 70 bpm as data under rest condition.

As shown the two set of ECG waveforms from different participants, Figs. 2 and 3, ECG waveforms from a certain individual change significantly before and after exercise. For different individuals, changes of their waveforms also manifest considerable differences, indicating ECG signals' uncertainty and bring great challenge to the accuracy of identification. However, the variations in two set of records share some simi-

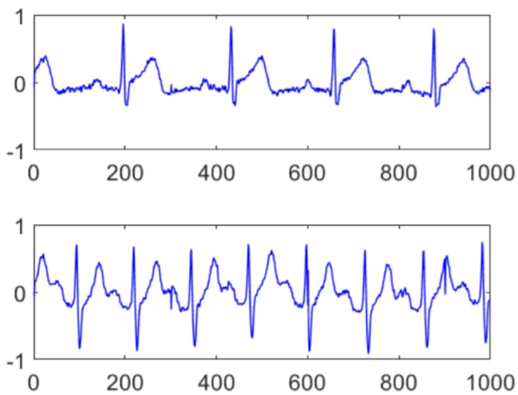

Fig. 3. Subject 2's ECG records before and after exercise.

larities; after exercise, heart rate increases, PR interval and QT interval are shortened, S wave becomes more salient, T wave is steeper, even approaching the peak of R wave whose amplitude also increases.

2.2. Preprocessing

The raw ECG signals were preprocessed through a fourth-order bandpass Butterworth filter with a cut-off frequencies of 0.5 Hz and 40 Hz [19]. Under 0.5 Hz, the signal is corrupted by baseline wander, while over 40 Hz, there will be distortion due to muscle movement, power-line noise etc.

2.3. Experiment on QRS complex

The experiment was mainly conducted in the following four scenarios: (1) training set and testing set are obtained from data before exercise(rest-rest ECGID), which is the most common application scenario; (2) the training set is from the first half of post-exercise recovery period, while testing set is from the second half of post-exercise recovery period (ex-ex ECGID I); (3) the training set is from the second half of post-exercise recovery period, and the test set is from the first half of post-exercise recovery period (ex-ex ECGID ii); (4) the training set is obtained from data before exercise, and the test set is from data after exercise (rest-ex ECGID). The fourth application scenario is the target application scenario of ECG identification studied in this paper while the first three application scenarios are serves as the comparison.

As mentioned before, QRS complex is the most stable part between rest and post-exercise, so we choose Pan & Tompkins algorithm to locate QRS complex. Since the length of QRS complex varies between 15 and 35 samples, we normalize the duration of QRS complex to the same periodic length based on the procedure presented in Wei et al. [37], that is, one of the ECG segments $\boldsymbol{y}_i$=$[y_i(1), y_i(2), \dots, y_i(n^*)]$ can be converted into a segment $\boldsymbol{x}_i$=$[x_i(1), x_i(2), \dots, x_i(n)]$ that holds the same signal morphology but in different data length (i.e., $n^* \neq n$) using the following equation,

$$x_i(j) = y_i(j^*) + (y_i(j^*+1) - y_i(j^*))(r_j - j^*), \tag{1}$$

where $r_j = (j-1)(n^*-1)/(n-1)+1$, and j^* is the integral part of r_j. The various lengths of the QRS complex will be compressed or extended into a set of ECG segments with the same periodic length. Let $n = 30$, therefore, these 30 samples will be considered as the main description of a heartbeat, that is, the features. As for the classification method, we choose RBF kernel with $c = 100$ and $\gamma = 1$ for SVM after reducing the feature dimension with PCA (Table 1).

2.4. Experiment on ECG beat

We utilize Pan & Tompkins algorithm to locate R peak and search the midpoints of two R-peak samples, between which is defined as a ECG

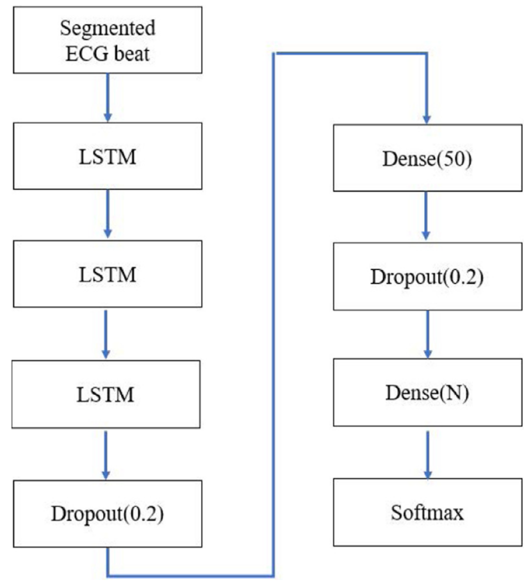

Fig. 4. Network structure of LSTM on ECGID.

segment. Similar to the method in the experiment on QRS complex, we apply the procedure presented in Ref. [37] to normalize the length of ECG segments. Let $n = 300$ here and these 300 samples are regarded as the features of a heartbeat. SVM and deep learning for classification are adopted respectively. The network structure of the latter is as shown in Fig. 4. And the results of experiment on ECG beat are shown in Tables 2 and 3:

2.5. Experiment on PQRST piecewise correction

In this experiment, we divide a complete heart beat into four parts: PQ segment, QRS segment, ST segment and T segment. After the detection of R peak, the location of R peaks is denoted as $R(i)$, $i = 1, 2, 3, \dots, m$. Since changes in heart rate are not evenly distributed in the P, R, and T complexes, piecewise correction on these segments are adopted as follows. PQ segment can be obtained using the following Equation [38],

$$PQ(i) = [R(i) - 230\ \text{ms} + dt]_s : [R(i) - 90\ \text{ms}]_s, \tag{2}$$

where $A : B$ means from A to B, $[\cdot]_s$ means the original ECG signal, dt is a variable threshold with changes in heart rate which can be described as follows,

$$dt = \begin{cases} -10\ \text{ms}, & HR < 65 \\ 0\ \text{ms}, & 65 \le HR < 80 \\ 10\ \text{ms}, & 80 \le HR < 95 \\ 20\ \text{ms}, & 95 \le HR < 110 \\ 30\ \text{ms}, & 110 \le HR < 125 \\ 40\ \text{ms}, & 125 \le HR < 140 \\ 50\ \text{ms}, & 140 \le HR < 155 \end{cases}. \tag{3}$$

QRS-segment can be obtained using Eq. (4)

$$QRS(i) = [R(i) - 90\ \text{ms}]_s : [R(i) + 100\ \text{ms}]_s. \tag{4}$$

ST-segment can be obtained using Eq. (5)

$$ST(i) = [R(i) + 100\ \text{ms}]_s : [R(i) + 100\ \text{ms} + 0.08 \times RR]_s, \tag{5}$$

where RR is the current RR interval. As for T-segment, it is described by Eq. (6)

$$T(i) = [R(i) + 100\ \text{ms} + 0.08 \times RR]_s : [R(i) + 0.42 \times RR]_s. \tag{6}$$

After wave correction, we use the method mentioned above to resample PQ segments to 450 ms length, ST segment to 110 ms length, and T segment to 50 ms length, while the QRS segment remains unchanged due

Table 1
ECGID performance on QRS complex .

Training set	Test set	Training accuracy	Test accuracy
rest record	rest record	98%	95%
post-exercise(first 70%)	post-exercise(last 30%)	94.1%	82.9%
post-exercise(last 70%)	post-exercise(first 30%)	94.8%	70.2%
rest	post-exercise	97.9%	17.5%

Table 2
ECGID performance on ECG beat with SVM.

Training set	Test set	Training accuracy	Test accuracy
rest record	rest record	100%	96.2%
post-exercise(first 70%)	post-exercise(last 30%)	100%	85.4%
post-exercise(last 70%)	post-exercise(first 30%)	100%	72.6%
rest	post-exercise	99.6%	2.7%

Table 3
ECGID performance on ECG beat with LSTM.

Training set	Test set	Training accuracy	Test accuracy
rest record	rest record	97.4%	95.6%
post-exercise(first 70%)	post-exercise(last 30%)	96%	82.3%
post-exercise(last 70%)	post-exercise(first 30%)	97.2%	77.6%
rest	post-exercise	98.2%	12%

Table 4
ECGID performance on PQRST piecewise correction.

Training set	Test set	Training accuracy	Test accuracy
rest record	rest record	100%	98.2%
post-exercise(first 70%)	post-exercise(last 30%)	100%	88%
post-exercise(last 70%)	post-exercise(first 30%)	100%	63.3%
rest	post-exercise	99.9%	4.9%

Table 5
ECGID performance on band pass filtering.

Training set	Test set	Training accuracy	Test accuracy
rest	rest	100%	92.7%
post-exercise(first 70%)	post-exercise(last 30%)	100%	85.4%
post-exercise(last 70%)	post-exercise(first 30%)	100%	52.4%
rest	post-exercise	98.6%	3%

to its fairly constancy. Then these segments are combined to recreate the entire heartbeat whose length is 800 ms normally. Besides, the amplitude of each new heartbeat is also normalized to a mean zero. Then, we perform two kinds of processing approaches. One is to directly classify the new heartbeat as a feature vector through PCA and SVM; the other is to extract the wavelet coefficient with the new heartbeat and then conduct identity classification. The experiment result is shown in Table 4:

2.6. Experiment on band pass filtering

Since Ref. [33] showed that the ECG waveform after exercise is similar to the rest one above 10 Hz, we filter the original ECG signal from 10 Hz to 40 Hz, including ones under rest and post-exercise situation, immediately after R peak detecting and ECG heartbeat segmentation. Then the heartbeats are resampled to 300 points length and rbf-SVM is used for classification. The experiment result is as follows (see Table 5):

2.7. Experiment on short-time Fourier transform

In this experiment, we use short-time Fourier transform [39,40] with Hamming window of the length 16 with step size of 13 computed over a 1 s window centered at R peak. The sampling frequency is 300 Hz, giving a total of 572 features. PCA is adopted for dimension reduction while rbf-SVM for classification. The experiment result is as follows (see Table 6):

2.8. Experiment on wavelet transform

After preprocessing, continuous wavelet transform [41] with 32 scales and Daubechies 5 as mother wavelet is computed on a 1 swindow centered at R peak, giving a total of 9600 features. Same as the above one, PCA is adopted for dimension reduction while rbf-SVM for classification. The experiment result is as follows (see Table 7):

2.9. Experiment on autocorrelation

Autocorrelation up to n lags is computed on windows of the length L seconds, where n and L are adjustable parameters. The experiment results are shown in Tables 8 and 9:

2.10. Experiment on feature selection

We randomly select half of the subjects (22 subjects) as an auxiliary data set and utilize the other half (23 subjects) for registration and testing. In other word, the first half is picked for feature selection while

Table 6
ECGID performance on STFT.

Training set	Test set	Training accuracy	Test accuracy
rest	rest	99.6%	98.3%
post-exercise(first 70%)	post-exercise(last 30%)	97.1%	75.3%
post-exercise(last 70%)	post-exercise(first 30%)	98.3%	66.1%
rest	post-exercise	99.6%	12.9%

Table 7
ECGID performance on wavelet transform.

Training set	Test set	Training accuracy	Test accuracy
rest	rest	99.9%	99.7%
post-exercise(first 70%)	post-exercise(last 30%)	99.8%	83%
post-exercise(last 70%)	post-exercise(first 30%)	99.9%	77.9%
rest	post-exercise	99.9%	7.1%

Table 8
ECGID performance on autocorrelation.

Training set	Test set	Training accuracy	Test accuracy
rest	rest	100%	93.8%
post-exercise(first 70%)	post-exercise(last 30%)	99.9%	74.3%
post-exercise(last 70%)	post-exercise(first 30%)	100%	60.1%
rest	post-exercise	90%	11.3%

Table 9
ECGID performance on beat with autocorrelation.

Training set	Test set	Training accuracy	Test accuracy
rest	rest	100%	95.2%
post-exercise(first 70%)	post-exercise(last 30%)	99.2%	67.3%
post-exercise(last 70%)	post-exercise(first 30%)	99.6%	63.9%
rest	post-exercise	98.3%	1.3%

the second one for calculating accuracy of identification where registration is performed in the resting state and testing in the post-exercise condition. We perform a short-time Fourier transform using a Hamming window of length 16 s with a step size of 13 to, and compute continuous wavelet transform with 32 scales and Daubechies 5 as mother wavelet over a window of length 1 s centered at R peak. Autocorrelation up to 80 lags is calculated over 1 s windows. In order to have zero mean and unit variance, every feature has to be normalized by z-score in the feature set which is collected by 10,252 features.

The feature selection is based on Kullback–Leibler (KL) divergence. Following Ref. [34], feature weights, $w(l)$, which measure the importance of a feature to rest-ex ECGID, are defined as linear combination of two terms

$$w(l) = \lambda w_1(l) - (1-\lambda) w_2(l). \tag{7}$$

The first term $w_1(l)$ related to the class separability is defined as follows

$$w_1(l) = \frac{1}{N}\sum_{i=1}^{N} d(f(X_i(l)), f(\chi(l))), \tag{8}$$

where $f(X_i(l))$ is probability density function(pdf) of lth feature computed over all samples of ith subject including both rest and post-exercise samples. $f(\chi(l))$ is pdf of lth feature computed over all samples of the auxiliary data set while N is total number of its subjects. $d(\cdot)$ is the symmetric KL divergence which can be estimated under a normal distribution as follows

$$d(f_1, f_2) = \frac{\sigma_1^2 + (\mu_1-\mu_2)^2}{2\sigma_2^2} + \frac{\sigma_2^2 + (\mu_1-\mu_2)^2}{2\sigma_1^2} - 1. \tag{9}$$

The second term in equation (13) related to the sensitivity of a feature to exercise is defined as below

$$\begin{aligned} w_2(l) = \frac{1}{N}\sum_{i=1}^{N} (d(f(X_i^{rest}(l)), f(X_i(l))) \\ + d(f(X_i^{post-ex}(l)), f(X_i(l)))), \end{aligned} \tag{10}$$

where $f(X_i^{rest}(l))(f(X_i^{post-ex}(l)))$ is part of 1th feature of subject i in rest(post-exercise) condition. $w_2(l)$ is small when the distribution corresponding to rest and post-exercise condition overlap with each other, suggesting the feature is more robust against exercise. Features can be selected by comparing the weights with a threshold and further sorted in descending order according to their weights, after which the top n features are picked. λ is chosen to be 0.3 empirically. The ECGID performance on KL feature selection is shown in Table 10, while the details of rest-ex ECGID performance is shown in Fig. 5.

Although KL feature selection method can significantly improve the rest-ex ECGID accuracy when compared to other methods, it is only 61.4%, far from satisfying the expectation.

2.11. Analysis on experiment results

From the results of applying different feature extraction and selection methods, it can be seen that, for the first scenario where both training and testing set are obtained from data before exercise(rest-rest ECGID), all methods experimented above can reach a test accuracy more than 90% while in the second and third ones where both sets are selected from post-exercise in different proportions, the test accuracy of each method reduces to varying degree. However, in the case of the forth scenario, simple feature extraction has been completely failed with a test accuracy less than 20%, except the KL feature selection whose accuracy is 61.4%. It is worth mentioning that a 50% accuracy given by a random

Table 10
ECGID performance on KL feature selection.

Training set	Test set	Training accuracy	Test accuracy
rest	rest	98.2%	93.8%
post-exercise(first 70%)	post-exercise(last 30%)	95.7%	85.1%
post-exercise(last 70%)	post-exercise(first 30%)	96.4%	73.9%
rest	post-exercise	98.7%	61.4%

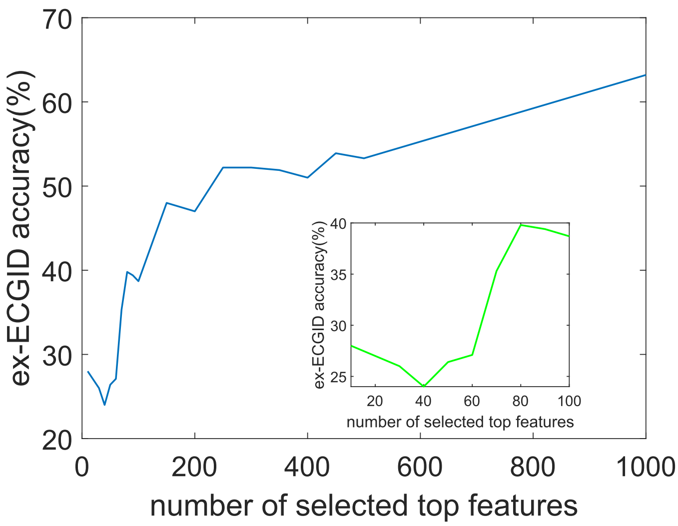

Fig. 5. Rest-ex ECGID accuracy of KL feature selection.

selection only occurs in the case of binary classification, while in the experiment of multi-classification, an accuracy less than 50% is possible and extremely common.

Since the training accuracy columns included in our tables rules out the possibility that the training classifiers are somewhat problematic, it can be demonstrated that it is the low generalization ability resulting in the unsatisfying classification performance on testing samples, in other words, the established algorithms cannot applied well in post-exercise data. In fact, exercise has a great impact on the ECG signal whose waveform remains unstable even during the recovery period after exercise, which can be verified based on both statistical results and the figures of ECG waveform.

3. Conclusion

In this manuscript, we focus on the influence of exercise on ECGID and apply existing machine learning methods to analyze the performance of rest-ex ECGID with our own ECG database. Through multiple sets of experiments, it is found that for current methods, the rest-rest ECGID accuracy can reach more than 95% while the ex-ex ECGID accuracy is a little lower. As for the rest-ex ECGID performance, most methods collapse to 10% or even worse, except for the KL feature selection method which can reach around 65%. Although KL feature selection method performs much better when compared with others, its result still remains unsatisfactory. In the future, researches might overcome the current oversimplified problem regarding rest-ex ECGID and develop more sophisticated feature selection algorithms or obtain more stable features by filtering out the part with violent changes due to exercise. Furthermore, other more advanced methods in the field of identity recognition can be developed to improve the accuracy of rest-ex ECGID.

Declaration of Competing Interest

The authors declare that they have no known competing financial interests or personal relationships that could have appeared to influence the work reported in this paper.

Acknowledgments

This work was supported by the National Natural Science Foundation of China under Grant 61873317, and in part by the Guangdong Basic and Applied Basic Research Foundation under Grant 2020A1515011375.

References

[1] A.K. Jain, A. Ross, S. Prabhakar, An introduction to biometric recognition, IEEE Trans. Circuits Syst. Video Tech. 14 (1) (2004) 4–20.
[2] B. Pourbabaee, M.J. Roshtkhari, K. Khorasani, Deep convolutional neural networks and learning ECG features for screening paroxysmal atrial fibrillation patients, IEEE Trans. Syst. Man Cybern. 48 (12) (2018) 2095–2104.
[3] K.A. Sidek, I. Khalil, H.F. Jelinek, ECG biometric with abnormal cardiac conditions in remote monitoring system, IEEE Trans. Syst. Man Cybern. 44 (11) (2014) 1498–1509.
[4] A. Bera, D. Bhattacharjee, Human identification using selected features from finger geometric profiles, IEEE Trans. Syst. Man Cybern. 50 (3) (2020) 747–761.
[5] R. Silipo, C. Marchesi, Artificial neural networks for automatic ECG analysis, IEEE Trans. Signal Process. 46 (5) (1998) 1417–1425.
[6] Y. Wang, K.N. Plataniotis, D. Hatzinakos, Integrating analytic and appearance attributes for human identification from ECG signal, in: Proc. Biometrics Symposiums, Baltimore, USA, 2006, p. 9677799.
[7] F. Agrafioti, D. Hatzinakos, ECG biometric analysis in cardiac irregularity conditions, Signal Image Video Process. 3 (4) (2009) 329–343.
[8] E. Bak, G.H. Choi, S.B. Pan, ECG-based human identification system by temporal-amplitude combined feature vectors, IEEE Access 8 (2020) 42217–42230.
[9] R. Hoekema, G.J.H. Uijen, A. van Oosterom, Geometrical aspects of the interindividual variability of multilead ECG recordings, IEEE Trans. Biomed. Eng. 48 (5) (2001) 551–559.
[10] L. Biel, O. Petterson, L. Philipson, P. Wide, ECG analysis: a new approach in human identification, IEEE Trans. Instrum. Meas. 50 (3) (2001) 808–812.
[11] F.M. Bui, D. Hatzinakos, Biometric methods for secure communications in body sensor networks: resource-efficient key management and signal-level data scrambling, EURASIP J. Adv. Signal Process. 2008 (2008) 529879.
[12] A.D.C. Chan, M.M. Hamdy, A. Badre, V. Badee, Person identification using electrocardiograms, in: Proc. Canadian Conference on Electrical and Computer Engineering, 2006, pp. 1–4.
[13] A real time ECG signal, Available: http://www.todayifoundout.com/index.php/2011/10/how-to-read-an-ekg-electrocardiograph/.
[14] Y. Li, W. Cui, Identifying the mislabeled training samples of ECG signals using machine learning, Biomed. Signal Process. Control 47 (2019) 168–176.
[15] S.S. Abdeldayem, T. Bourlaid, A novel approach for ECG-based human identification using spectral correlation and deep learning, IEEE Trans. Biom. Behav. Identity Sci. 2 (1) (2020) 1–14.
[16] R. Cordeiro, D. Gajaria, A. Limaye, T. Adegbija, N. Karimian, F. Tehranipoor, ECG-based authentication using timing-aware domain-specific architecture, IEEE Trans. Comput. Aided Design Integr. Circuits Syst. 39 (11) (2020) 3373–3384.
[17] T.W. Shen, W.J. Tompkins, Y.H. Hu, One-lead ECG for identity verification, in: Proc. The 2nd Joint Engineering in Medicine and Biology, 24th Annual Conference and the Annual Fall Meeting of the Biomedical Engineering Society, 2002, pp. 62–63.
[18] K.N. Platanioatis, D. Hatzinakos, J.K.M. Lee, ECG biometric recognition without fiducial detection, in: Proceedings of Biometrics Symposium: Special Session on Research at the Biometric Consortium Conference, 2006, pp. 19–21.
[19] Y. Wang, F. Agrafioti, D. Hatzinakos, K.N. Plataniotis, Analysis of human electrocardiogram for biometric recognition, EURASIP J. Adv. Signal Process. 2008 (2007) 148658.
[20] F. Agrafioti, D. Hatzinakos, ECG based recognition using second order statistics, in: Proc. Communication Networks and Services Research Conference, 2008, pp. 82–87.
[21] F. Agrafioti, D. Hatzinakos, ECG biometric analysis in cardiac irregularity conditions, Signal Image Video Process. 3 (4) (2009) 329–343.
[22] Q. Zhang, D. Zhou, X. Zeng, HeartID: a multiresolution convolutional neural network for ECG-based biometric human identification in smart health applications, IEEE Access 5 (2017) 11805–11816.

[23] The MIT-BIH arrhythmia database, Available: http://www.physionet.org/physiobank/database/mitdb/.
[24] The PTB diagnostic ECG database, national metrology institute of germany, Available: http://www.physionet.org/physiobank/database/ptbdb/.
[25] M.L. Simmons, P.G. Hugenholtz, Gradual changes of ECG waveform during and after exercise in normal subjects, Circulation 52 (1975) 570–577.
[26] A.L. Goldberger, V. Bhargava, Effect of exercise on QRS duration in healthy men: a computer ECG analysis, J. Appl. Physiol. Respir. Environ. Exerc. Physiol. 54 (4) (1983) 1083–1088.
[27] T.H. Hijzen, J.L. Slangen, The electrocardiogram during emotional and physical stress, Int. J. Psychophysiol. 2 (4) (1985) 273–279.
[28] J.W. Deckers, R.V. Vinke, J.R. Vos, M.L. Simoons, Changes in the electrocardiographic response to exercise in healthy women, Br. Heart J. 64 (6) (1990) 376–380.
[29] K.S. Kim, T.H. Yoon, J.W. Lee, D.J. Kim, H.S. Koo, A robust human identification by normalized time-domain features of electrocardiogram, in: Proc. IEEE Engineering in Medicine and Biology 27th Annual Conference, 2005, pp. 1114–1117.
[30] F. Porée, J.Y. Bansard, G. Kervio, G. Carrault, Stability analysis of the 12-lead ECG morphology in different physiological conditions of interest for biometric applications, Comput. Cardiol. 36 (2009) 285–288.
[31] J. Piao, J. Im, J. Han, Y. Yoon, Individual identification after exercise using a discrete wavelet transform of the ECG signal, in: Proc. General Conference of Korea Telecommunications Society, 2016, pp. 756–757.
[32] D. Sung, J. Kim, M. Koh, K. Park, ECG authentication in post-exercise situation, in: Proc. of the 39th International Conference of the IEEE Engineering in Medicine and Biology Society, 2017, pp. 446–449.
[33] T. Nobunaga, H. Tanaka, I. Tanahashi, T. Watanable, Y. Hattori, Optimised band–pass filter to ensure accurate ECG-based identification of exercising human subjects, Electron. Lett. 53 (4) (2017) 222–224.
[34] M. Komeili, W. Louis, N. Armanfard, D. Hatzinakos, On evaluating human recognition using electrocardiogram signals: from rest to exercise, in: Proc. IEEE Canadian Conference on Electrical and Computer Engineering, 2016, p. 16443965.
[35] S.C. Wu, P.L. Hung, A.L. Swindlehurst, ECG biometric recognition: unlinkability, irreversibility, and security, IEEE Internet Things J. 8 (1) (2021) 487–500.
[36] https://github.com/feimadada/exercise-ECGID-database-.
[37] J.J. Wei, C.J. Chang, N.K. Chou, G.J. Jan, ECG data compression using truncated singular value decomposition, IEEE Trans. Inf. Technol. Biomed. 5 (4) (2001) 290–299.
[38] Y. Zhang, Z.B. Xiao, Biometric identification method for ECG based on wavelet transform and piecewise correction, in: 2017 IEEE International Conference on Signal Processing, Communications and Computing, 2017, doi:10.1109/ICSPCC.2017.8242582.
[39] S.H. Nawab, T.F. Quatieri, J.S. Lim, Signal reconstruction from short-time fourier transform magnitude, IEEE Trans. Acoust. Speech Signal Process. 31 (4) (1983) 986–998.
[40] D.W. Griffin, J.S. Lim, Signal estimation from modified short-time fourier transform, IEEE Trans. Acoust. Speech Signal Process. 32 (2) (1984) 236–243. Apr.
[41] Y. Li, W.G. Cui, Y.Z. Guo, T. Huang, X.F. Yang, H.L. Wei, Time-varying system identification using an ultra-orthogonal forward regression and multiwavelet basis functions with applications to EEG, IEEE Trans. Neural Netw. Learn. Syst. 29 (7) (2018) 2960–2972.